Supporting Information for

"Constraints on transient viscoelastic rheology of the asthenosphere from seasonal deformation"

Kristel Chanard[1,2,3], Luce Fleitout [2], Eric Calais [2], Sylvain Barbot[4] and Jean-Philippe Avouac[3]

[1]LASTIG LAREG, IGN, ENSG, Université Paris Diderot, Sorbonne Paris Cité, Paris, France

[2]Laboratoire de Géologie, CNRS UMR 8538, École normale Supérieure, PSL Research University, Paris, France

[3]Division of Earth and Planetary Sciences, California Institute of Technology, Pasadena, USA

[4]Department of Earth Sciences, University of Southern California, Los Angeles, USA

Contents

- Figures S1 to S6

References

Bassin, C. (2000), The current limits of resolution for surface wave tomography in north america, *Eos Trans. AGU*.

Chanard, K. (2015) Seasonal deformation of the Earth, impact on seismicity *Ph.D., École Normale Supérieure, Paris, France*

Dziewonski, A., and D. Anderson (1981), Preliminary reference Earth model, *Physics of the Earth and Planetary Interiors*, *25*, 297–356.

Figures

Corresponding author: Kristel Chanard, kristel.chanard@ign.fr

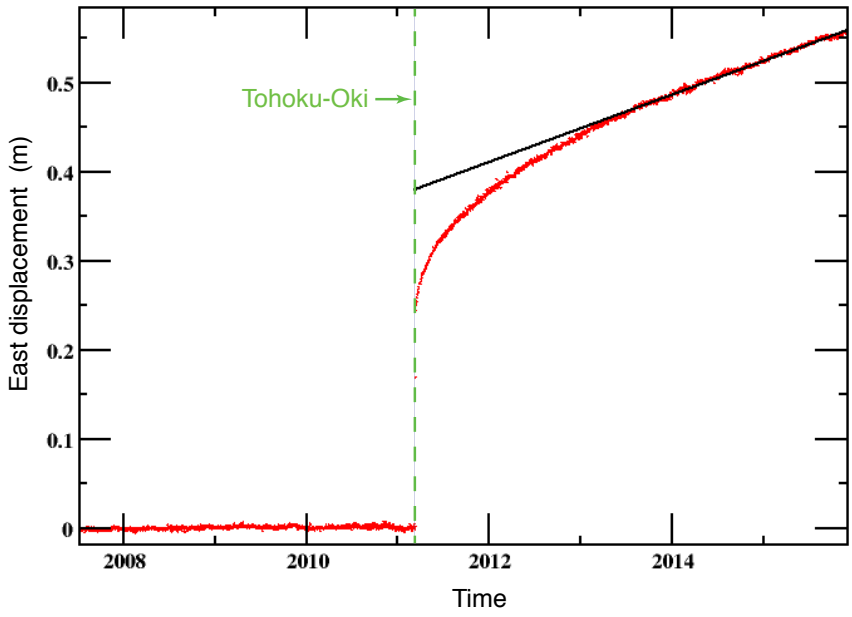

Figure 1. Daily GPS positions featuring co and postseismic east displacements due to Tohoku earthquake at station J252 (Japan, see location on Figure S2, 500km away from the Tohoku Oki epicenter). The slope of the postseismic displacement a few years after the earthquake (black line), can be explained by viscoelastic relaxation in an asthenosphere with an apparent viscosity of 3×10^{18}Pa.s. Various mechanisms, including much faster viscoelastic relaxation have been proposed to explain the rapid displacement just after the earthquake.

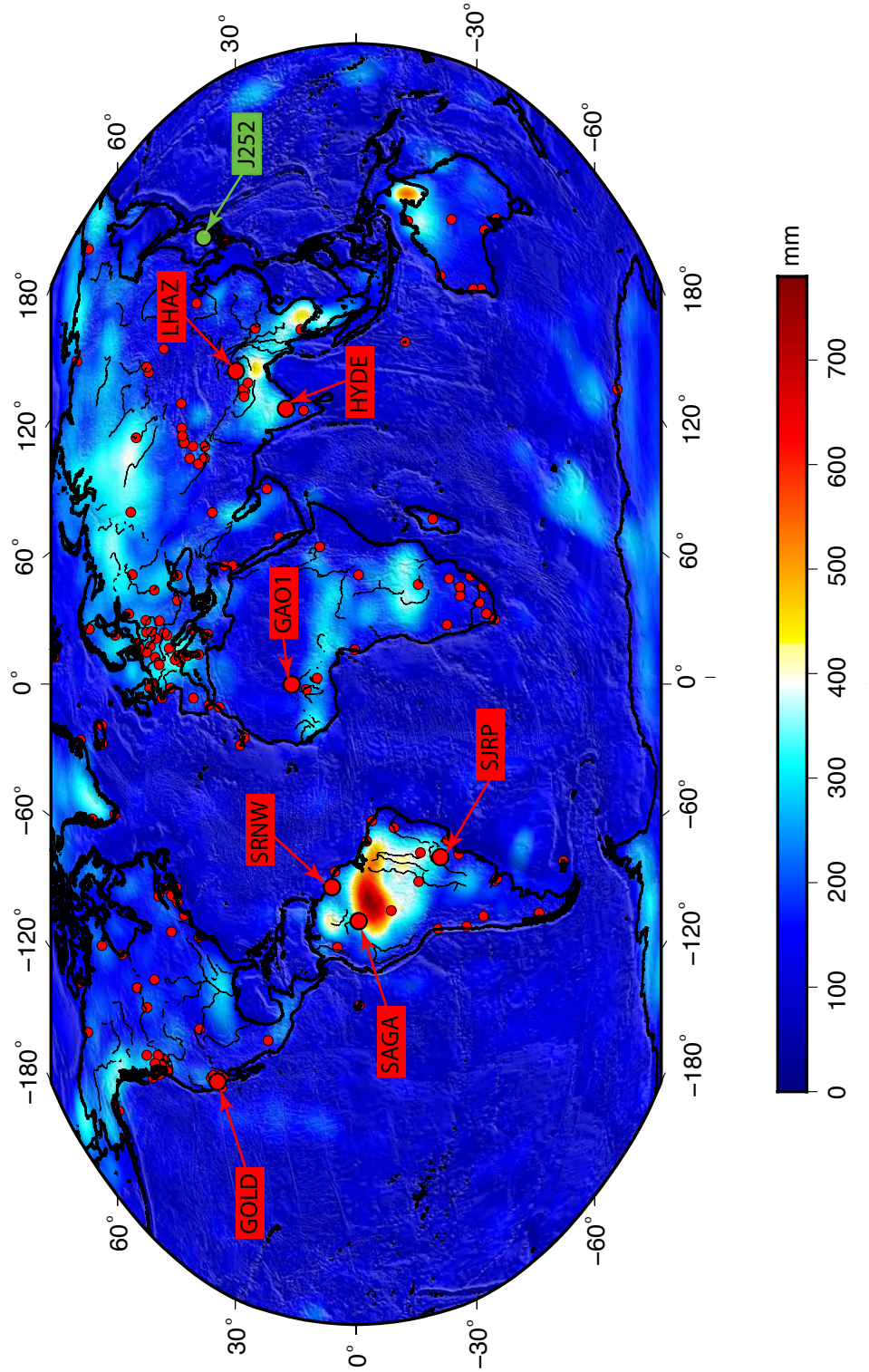

Figure 2. Peak to peak surface load variations, expressed in equivalent water height (in mm), derived from GRACE for the 2002-2012 period and corrected from detectable earthquakes coseismic contributions. Red dots show location of the continuous GPS stations used in this study. Locations of cGPS stations for which time series are shown on Figure S1 (green) and on Figure S6 (red) are highlighted.

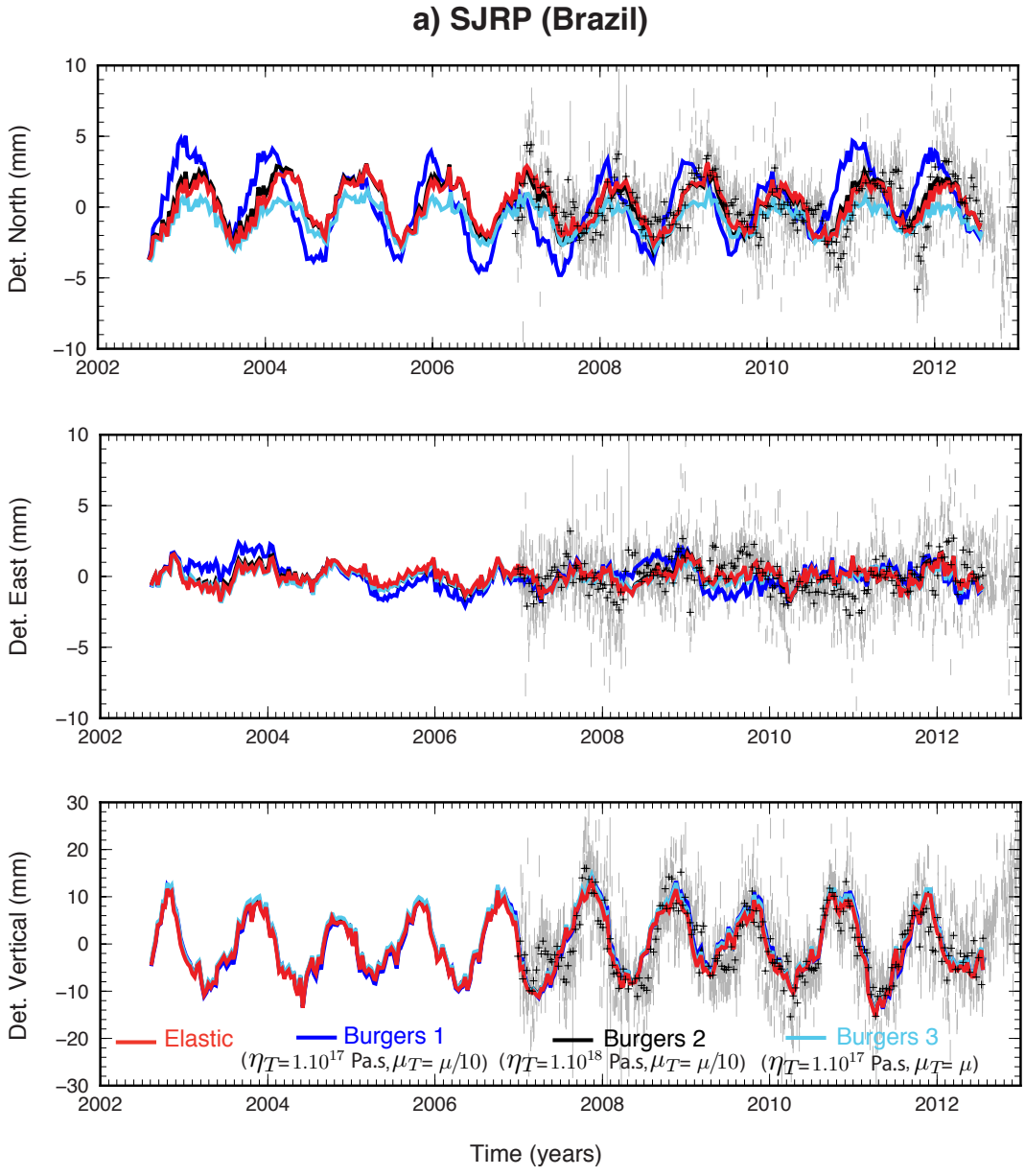
a) SJRP (Brazil)
Det. North (mm)
Det. East (mm)
Det. Vertical (mm)
Time (years)
Elastic
Burgers 1
(η_T=1.10^{17} Pa.s, μ_T= μ/10)
Burgers 2
(η_T=1.10^{18} Pa.s, μ_T= μ/10)
Burgers 3
(η_T=1.10^{17} Pa.s, μ_T= μ)

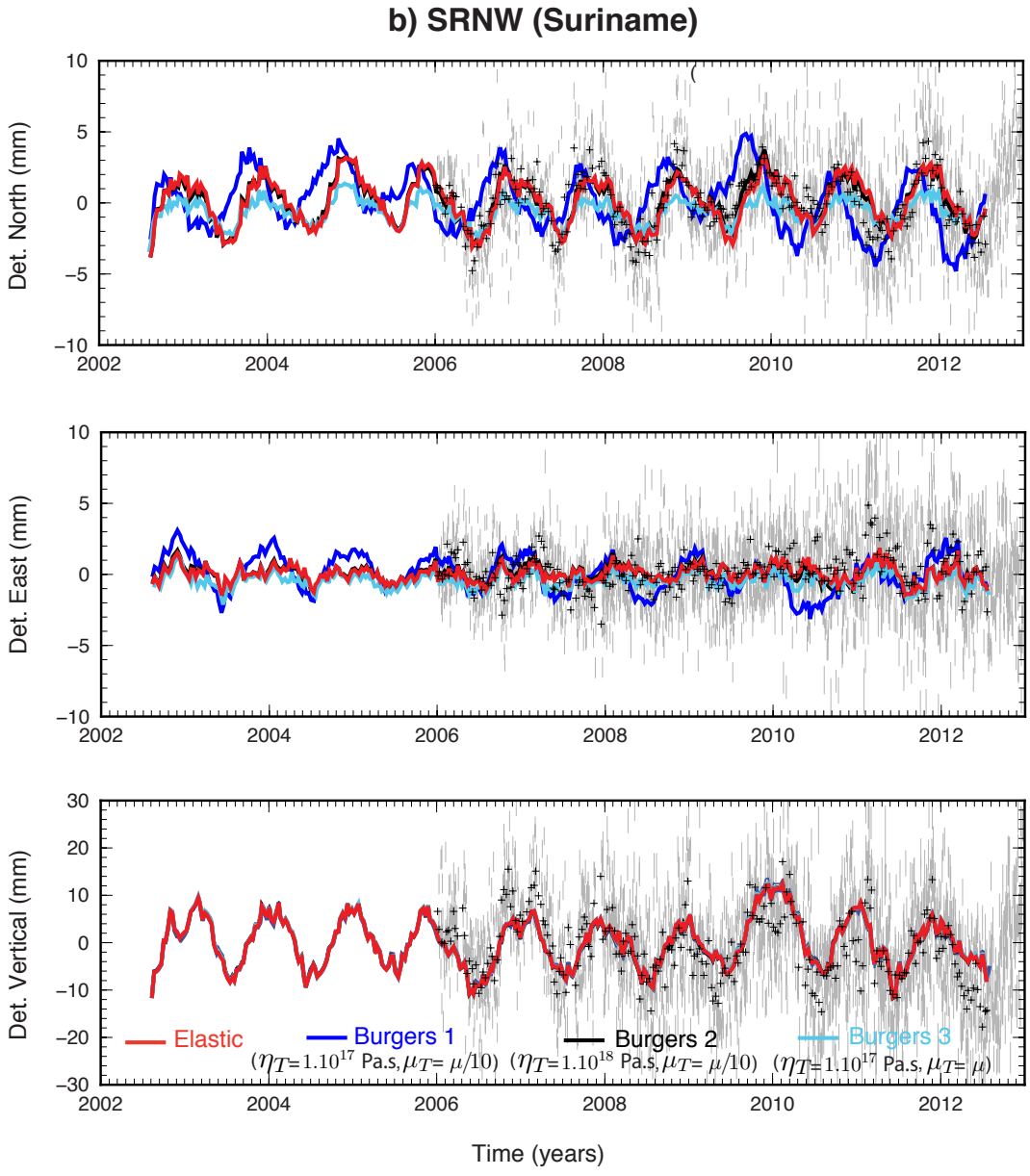
b) SRNW (Suriname)
Det. North (mm)
Det. East (mm)
Det. Vertical (mm)
Time (years)
Elastic
Burgers 1
(η_T=1.10^{17} Pa.s, μ_T= μ/10)
Burgers 2
(η_T=1.10^{18} Pa.s, μ_T= μ/10)
Burgers 3
(η_T=1.10^{17} Pa.s, μ_T= μ)

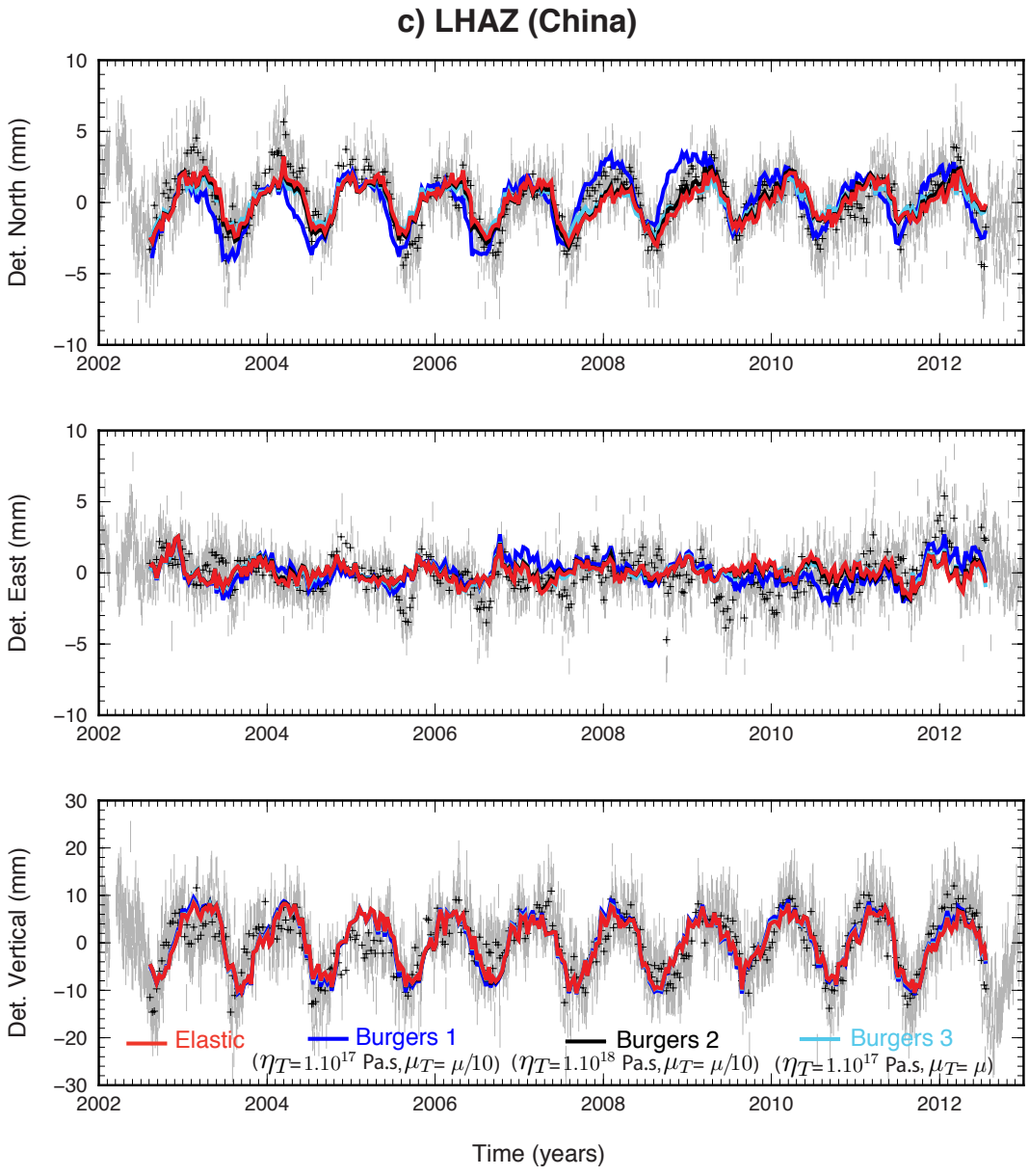
c) LHAZ (China)
Det. North (mm)
Det. East (mm)
Det. Vertical (mm)
Time (years)
Elastic
Burgers 1
(η_T=1.10^{17} Pa.s,μ_T= μ/10)
Burgers 2
(η_T=1.10^{18} Pa.s,μ_T= μ/10)
Burgers 3
(η_T=1.10^{17} Pa.s, μ_T= μ)

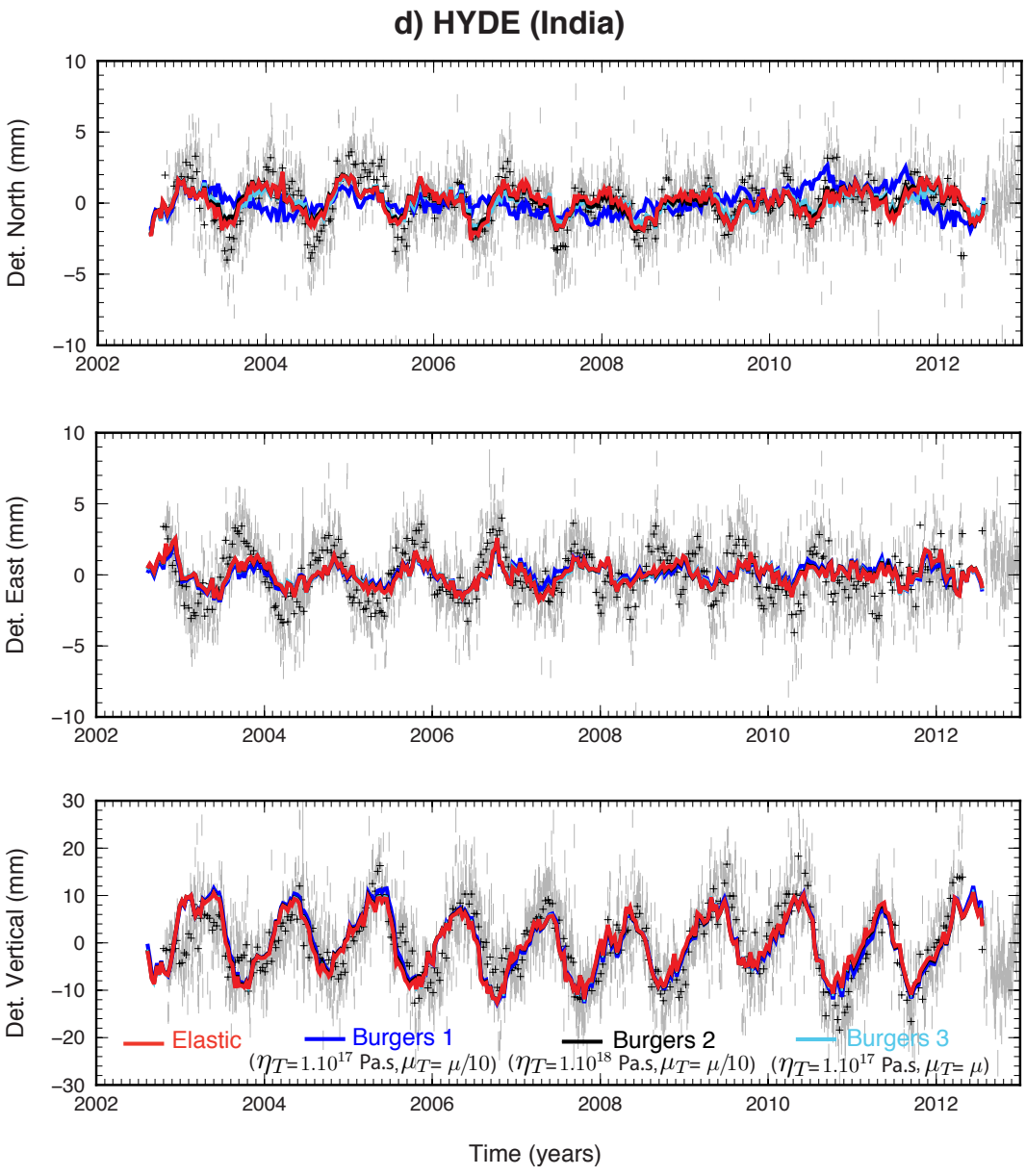
d) HYDE (India)
Det. North (mm)
Det. East (mm)
Det. Vertical (mm)
Time (years)
Elastic
Burgers 1
(η_T=1.10^{17} Pa.s,μ_T= μ/10)
Burgers 2
(η_T=1.10^{18} Pa.s,μ_T= μ/10)
Burgers 3
(η_T=1.10^{17} Pa.s, μ_T= μ)

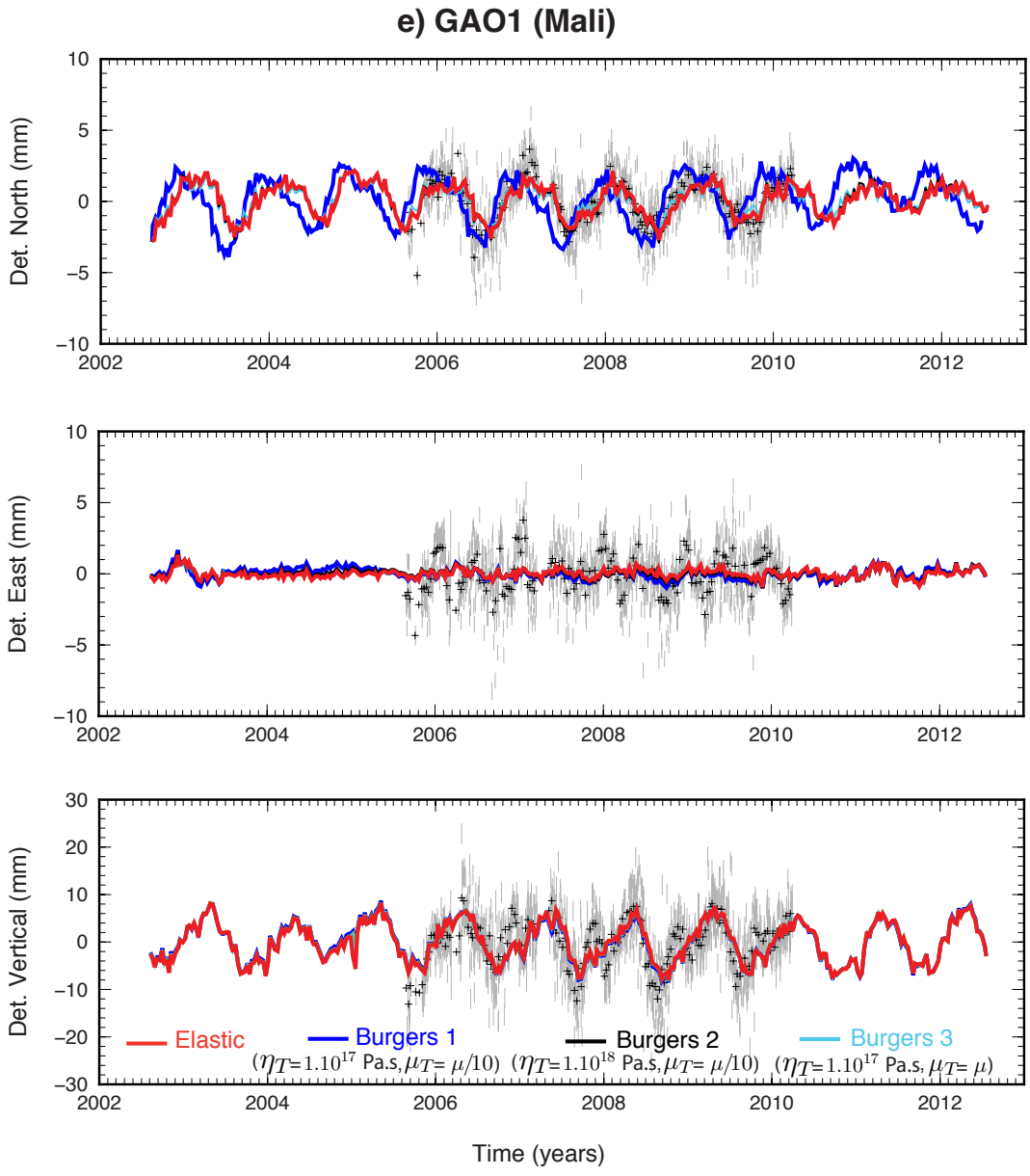
e) GAO1 (Mali)
Det. North (mm)
Det. East (mm)
Det. Vertical (mm)
Time (years)
Elastic
Burgers 1
(η_T=1.10^{17} Pa.s,μ_T= μ/10)
Burgers 2
(η_T=1.10^{18} Pa.s,μ_T= μ/10)
Burgers 3
(η_T=1.10^{17} Pa.s, μ_T= μ)

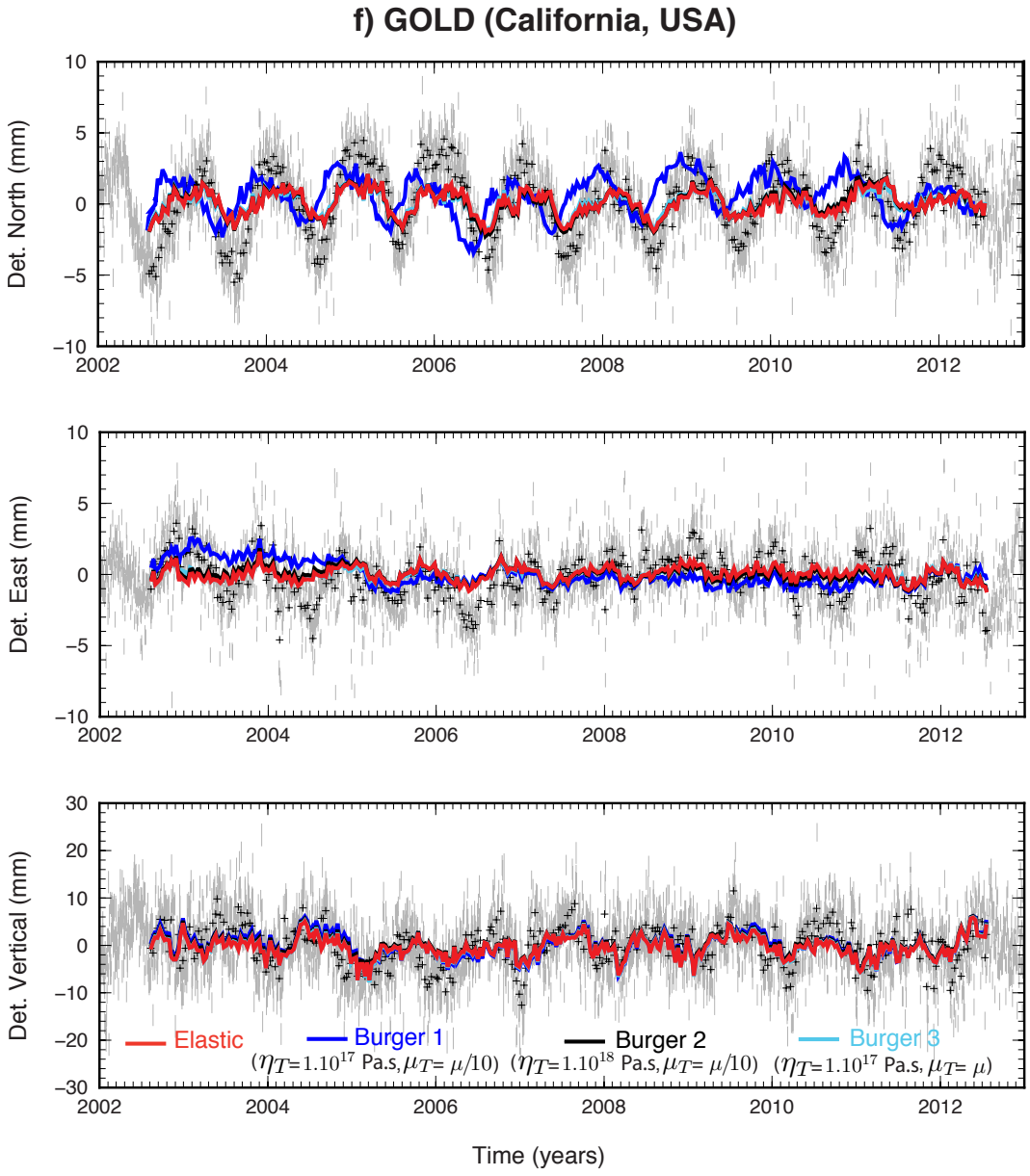

Figure 3. Daily detrended geodetic positions, error-bars for 1-σ uncertainties (gray) and 10-days moving-average (black) determined at a) SJRP, b) SRNW, c) LHAZ, d) HYDE, e) GAO1 and f) GOLD stations (location on Figure 2). Predicted displacements induced by GRACE derived seasonal surface loading derived are shown for a purely elastic model (red), Burgers 1 (blue) where $\eta_T = 1.10^{17}$, $\eta = 1.10^{19}$, $\mu_T = \mu/10$ between 70 and 270 km depth; Burgers 2 (black) where $\eta_T = 1.10^{18}$, $\eta = 1.10^{19}$, $\mu_T = \mu/10$ between 70 and 270 km depth; and Burgers 3 (light blue) where $\eta_T = 1.10^{17}$, $\eta = 1.10^{19}$, $\mu_T = \mu$ between 70 and 270 km depth. In all models, degree-1 and reference frame issues have been addressed as proposed by *Chanard* [2015].

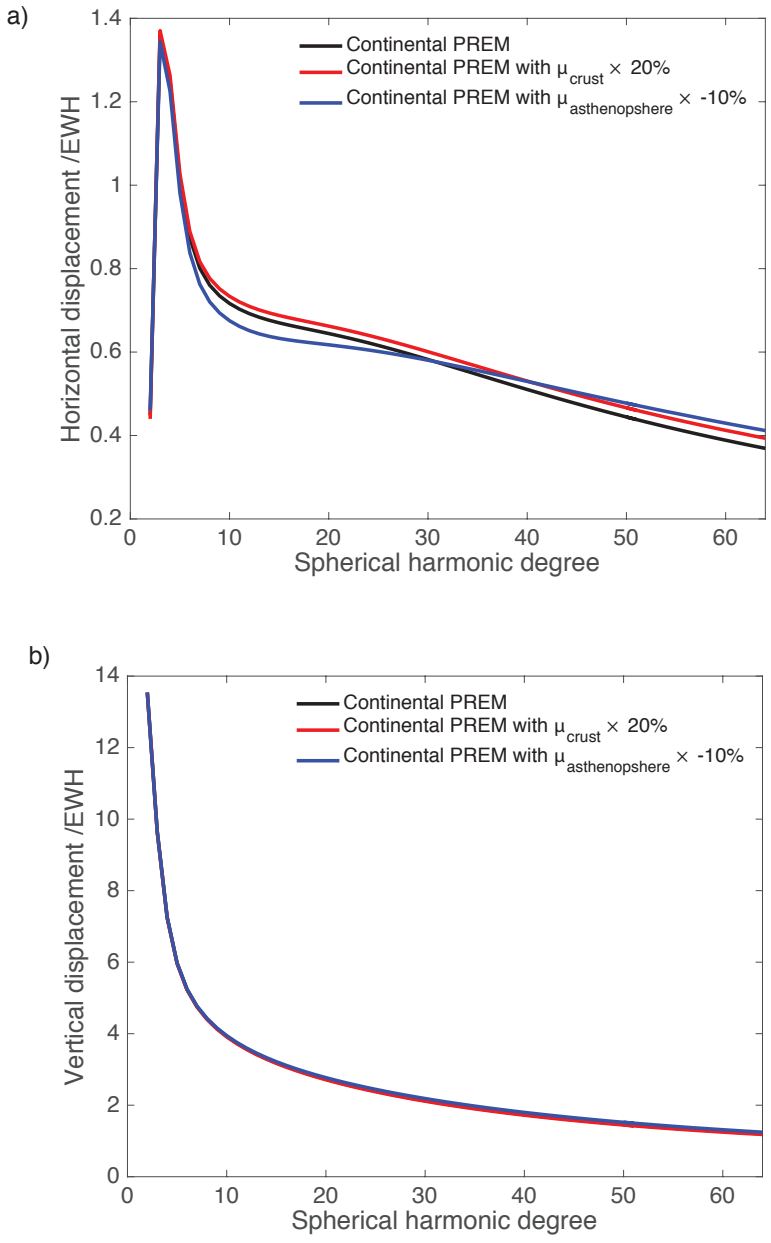

Figure 4. Horizontal (a) and vertical (b) amplitude of surface displacements as a function of spherical harmonic number, in response to a unit 1 year periodic unit harmonic loading function acting on spherical and layered models: the Preliminary Reference Earth model (PREM) proposed by *Dziewonski and Anderson* [1981] for which the ocean is replaced by a continental crust [*Bassin*, 2000] (black), the same model where the shear modulus in the crust (down to 40km) in increased by 20% (red) and another similar model where the shear modulus is reduced by 10% in the asthenosphere (70-270km) (blue).

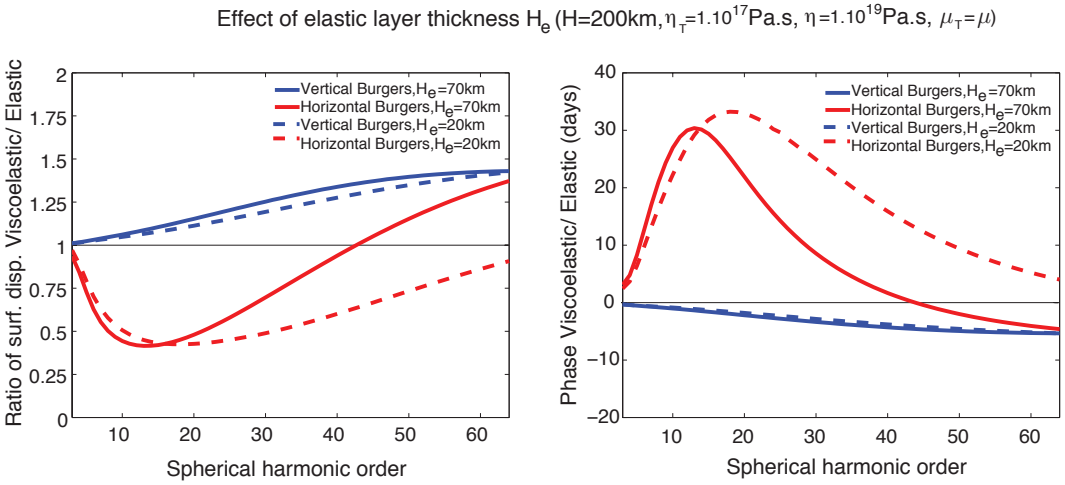

Figure 5. Ratio of surface displacements and phase lag between viscoelastic models with a Burgers asthenospheric rheologies and a purely elastic model for vertical (blue) and horizontal (red) components, induced by a 1-year periodic unit harmonic loading function obtained respectively using a viscoelastic model, showing the effect of of the surficial elastic layer overlying a viscoelastic asthenosphere on surface displacements.

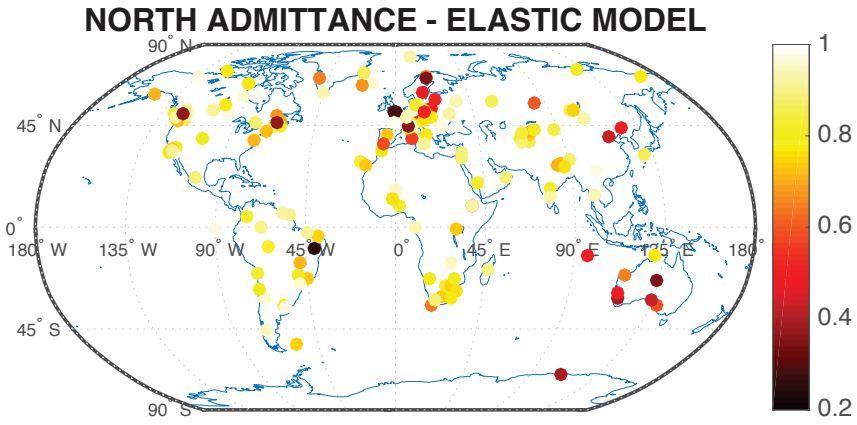
NORTH ADMITTANCE - ELASTIC MODEL
90° N
45° N
0°
180° W
135° W
90° W
45° W
0°
45° E
90° E
135° E
180°
45° S
90° S
1
0.8
0.6
0.4
0.2

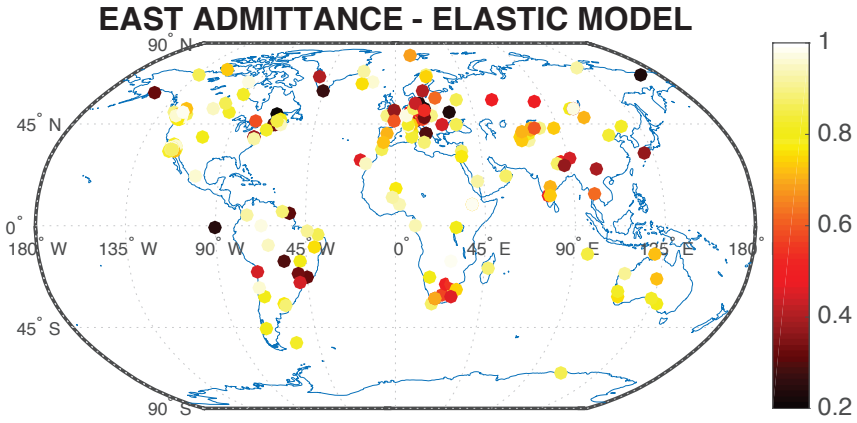
EAST ADMITTANCE - ELASTIC MODEL
90° N
45° N
0°
180° W
135° W
90° W
45° W
0°
45° E
90° E
135° E
180°
45° S
90° S
1
0.8
0.6
0.4
0.2

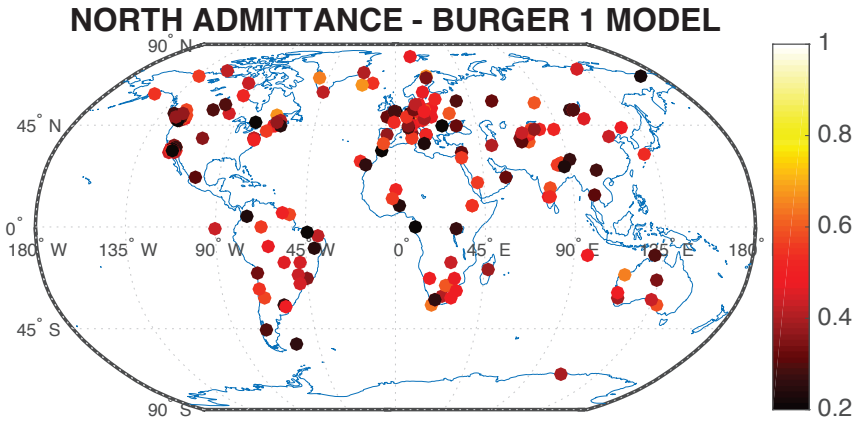
NORTH ADMITTANCE - BURGER 1 MODEL
90° N
45° N
0°
180° W
135° W
90° W
45° W
0°
45° E
90° E
135° E
180°
45° S
90° S
1
0.8
0.6
0.4
0.2

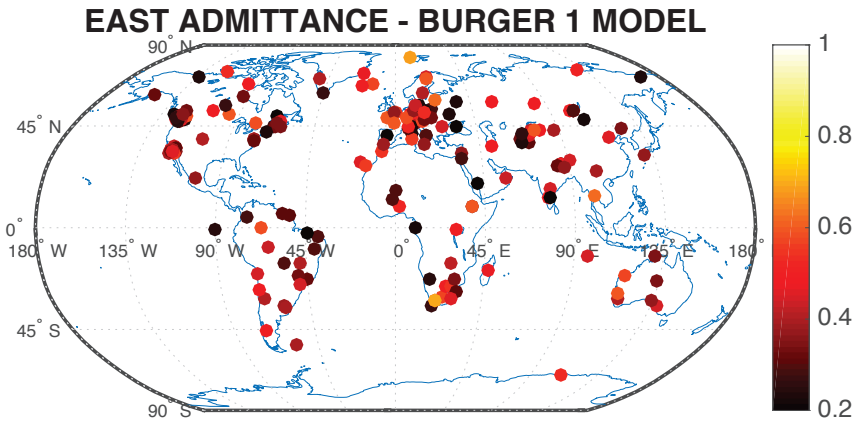
EAST ADMITTANCE - BURGER 1 MODEL
90° N
45° N
0°
180° W
135° W
90° W
45° W
0°
45° E
90° E
135° E
180°
45° S
90° S
1
0.8
0.6
0.4
0.2

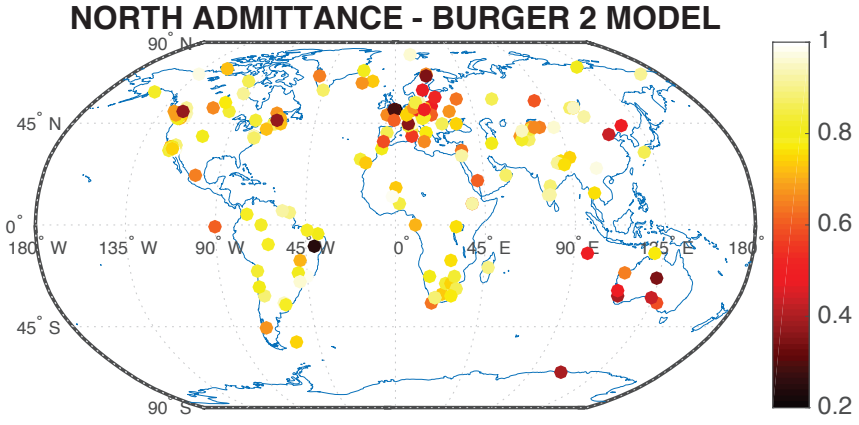
NORTH ADMITTANCE - BURGER 2 MODEL
90° N
45° N
0°
180° W
135° W
90° W
45° W
0°
45° E
90° E
135° E
180°
45° S
90° S
1
0.8
0.6
0.4
0.2

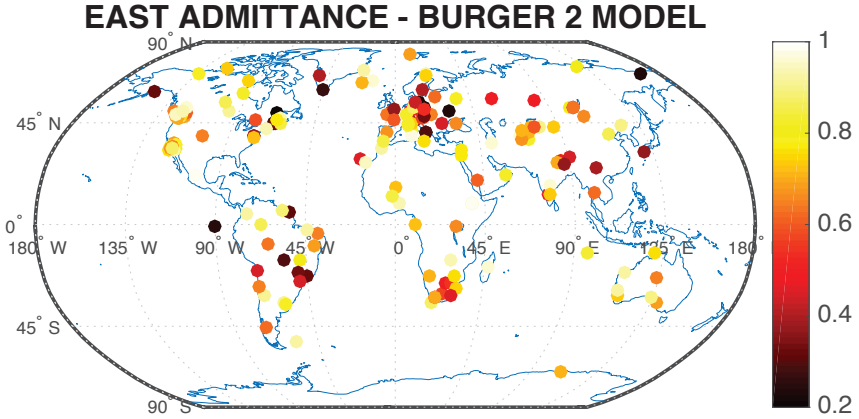
EAST ADMITTANCE - BURGER 2 MODEL
90° N
45° N
0°
180° W
135° W
90° W
45° W
0°
45° E
90° E
135° E
180°
45° S
90° S
1
0.8
0.6
0.4
0.2

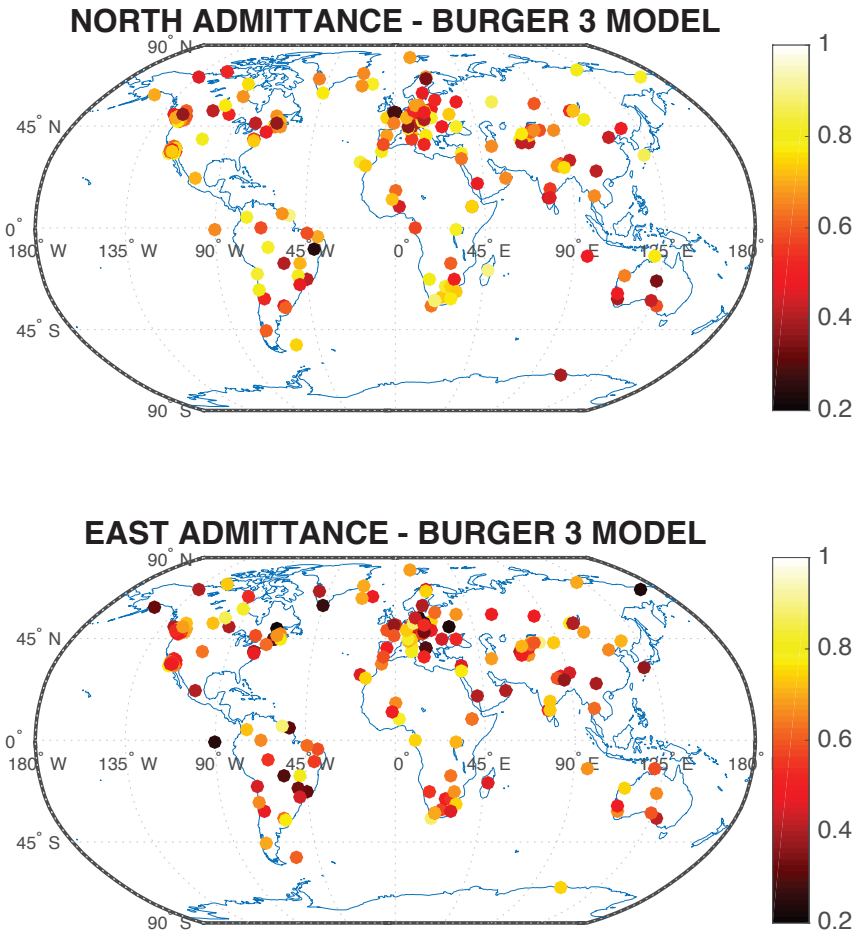

Figure 6. Maps of North and East admittance as defined by Equation 2 for a purely elastic model (a), Burgers 1 (b) where $\eta_T = 1.10^{17}$, $\eta = 1.10^{19}$, $\mu_T = \mu/10$ between 70 and 270 km depth; Burgers 2 (c) where $\eta_T = 1.10^{18}$, $\eta = 1.10^{19}$, $\mu_T = \mu/10$ between 70 and 270 km depth; and Burgers 3 (d) where $\eta_T = 1.10^{17}$, $\eta = 1.10^{19}$, $\mu_T = \mu$ between 70 and 270 km depth. In all models, degree-1 and reference frame issues have been addressed as proposed by *Chanard* [2015]. Model parameters are summarized in Table 1.